On the evaluation of groundwater contamination from underground nuclear tests

A.F.B. Tompson · C.J. Bruton · G.A. Pawloski · D.K. Smith · W.L. Bourcier
D.E. Shumaker · A.B. Kersting · S.F. Carle · R.M. Maxwell

Abstract Increasing concern about radioactive contamination of groundwater from underground nuclear tests has reinforced the need for a basic understanding of how the radionuclide inventories of such tests enter and migrate through groundwater. As a basis for studying these processes, the physically and thermally disturbed geologic environment produced by such tests and its relation to the post-test distribution of radionuclides is discussed from a conceptual perspective. These concepts are used to support the development of a reactive transport model to evaluate the nature and extent of radionuclide contamination within alluvium surrounding a specific underground nuclear test at the Nevada Test Site (NTS). Simulations are focused on determining the abundance and chemical nature of radionuclides that are introduced into groundwater, as well as the rate and extent of radionuclide migration and reaction in groundwater surrounding the working point of the test. Transport simulations based upon a streamline-based numerical model are used to illustrate the nature of radionuclide elution out of the near-field environment and illustrate the conceptual modeling process. The numerical approach allowed for relatively complex flow and chemical reactions to be considered in a computationally efficient manner. The results are particularly sensitive to the rate of melt glass dissolution, distribution of reactive minerals in the alluvium, and overall groundwater flow configuration. They provide a rational basis from which defensible migration assessments over larger spatial and temporal scales can proceed.

Keywords Contamination · Groundwater · Nuclear testing · Nevada Test Site · Radioactive

Received: 10 June 2001 / Accepted: 10 September 2001
Published online: 13 February 2002

A.F.B. Tompson (✉) · C.J. Bruton · G.A. Pawloski
W.L. Bourcier · S.F. Carle · R.M. Maxwell
Geosciences and Environmental Technologies Division,
Lawrence Livermore National Laboratory,
Livermore, CA 94551, USA
E-mail: afbt@llnl.gov

D.E. Shumaker
Center for Applied Scientific Computing,
Lawrence Livermore National Laboratory,
Livermore, CA 94551, USA

D.K. Smith · A.B. Kersting
Analytical and Nuclear Sciences Division,
Lawrence Livermore National Laboratory,
Livermore, CA 94551, USA

Introduction

There is increasing concern about the environmental risks posed by radionuclides produced by underground nuclear tests (USDOE 1997a; IAEA 1998a, 1998b, 1998c). These risks are dependent, in large part, on the physical and chemical mechanisms that control how radionuclides are introduced and transported in groundwater to various receptors in the biosphere. In southern Nevada and other continental testing locations in the USA, environmental concerns include the potential contamination of groundwater and its effect on domestic or agricultural uses, as well its ultimate discharge into surface water supplies where collateral ecological impacts may occur (USDOE 1997a). In the oceanic testing regions in the South Pacific and Aleutian Islands, additional concerns arise with respect to radionuclide seepage from groundwater into seawater and its subsequent effects on fisheries and related ecologies (e.g., IAEA 1998b, 1998c).

Over 800 nuclear tests were conducted underground at the Nevada Test Site (NTS), of which, roughly a third were located beneath the water table (USDOE 1997b, 2000). The radionuclide inventory of below-water table tests alone currently includes over 10^8 curies (Ci) of radioactivity (Wild and others 1998). As most underground testing locations are hundreds of meters or more beneath the ground surface, they are difficult to gain access to for characterization purposes, much less for removing radioactive contaminants, or assessing their tendency to move towards public or private wells. As a result, the assessment of the potential for test-related radionuclides to enter and move through groundwater has tended to rely heavily on the use of computer simulations (Ogard and others 1988,

USDOE 1997a; IAEA 1998b; Pohll and others 1999; Tompson and others 1999; Glascoe and others 2000; Maxwell and others 2000). Although such models are designed to better understand the complex mechanisms involved in radionuclide release and migration, they serve equally well in interpreting and integrating the modicum of specific data that do exist (e.g., Borg and others 1976; Hoffman and others 1977; Bryant 1992; Smith 1995; Thompson 1996; IAEA 1998a; Kersting and others 1999; Sawyer and others 1999). They are also useful for designing data acquisition strategies for future validation and characterization purposes.

In this paper, we review several of the more unique and pertinent steps required in such modeling studies, with a focus on the near-field "disturbed" environment surrounding a below-water table test. The first step in such an analysis is to understand the disturbed environment itself – how it was created and how the radiologic inventory is distributed about the working point of the test. Much of this discussion is conceptual in nature and involves a consideration of physical, chemical, and other complex shock-related (phenomenological) effects that are beyond the scope of traditional hydrologic flow and transport models. Following this, we will review what are believed to be the more important processes that relate how the radiologic inventory is ultimately translated into the aqueous regime and made available for transport away from the testing location. Finally, we will briefly review a set of streamline-based modeling simulations that are designed to approximate these processes and discuss implications for future work in this area.

Nuclear test effects

The detonation of an underground nuclear device releases an immense amount of energy that vaporizes the geologic and device-related materials in a local region surrounding the testing point (Germain and Kahn 1968; Borg and others 1976; US Congress 1989; IAEA 1998b). High temperatures and a compressive shock wave generated by the test will produce a cavity about the testing point and fracture or alter the formation beyond the cavity wall (Fig. 1; Pawloski 1999). The cavity volume is created by both vaporization and compression of the original geologic media. Molten rock or alluvium will coat the cavity wall. The size (or radius) of the cavity can be estimated as a function of the energy of the explosion, its depth of burial, and the strength of the geologic media (Borg and others 1976). The maximum cavity size is reached within about a tenth of a second after detonation. For tests conducted in the saturated zone, groundwater will be vaporized in the immediate cavity region, and a groundwater-mounding effect can be created further away that will eventually relax over time (Knox and others 1965; Borg and others 1976; Burkhard and Rambo 1991).

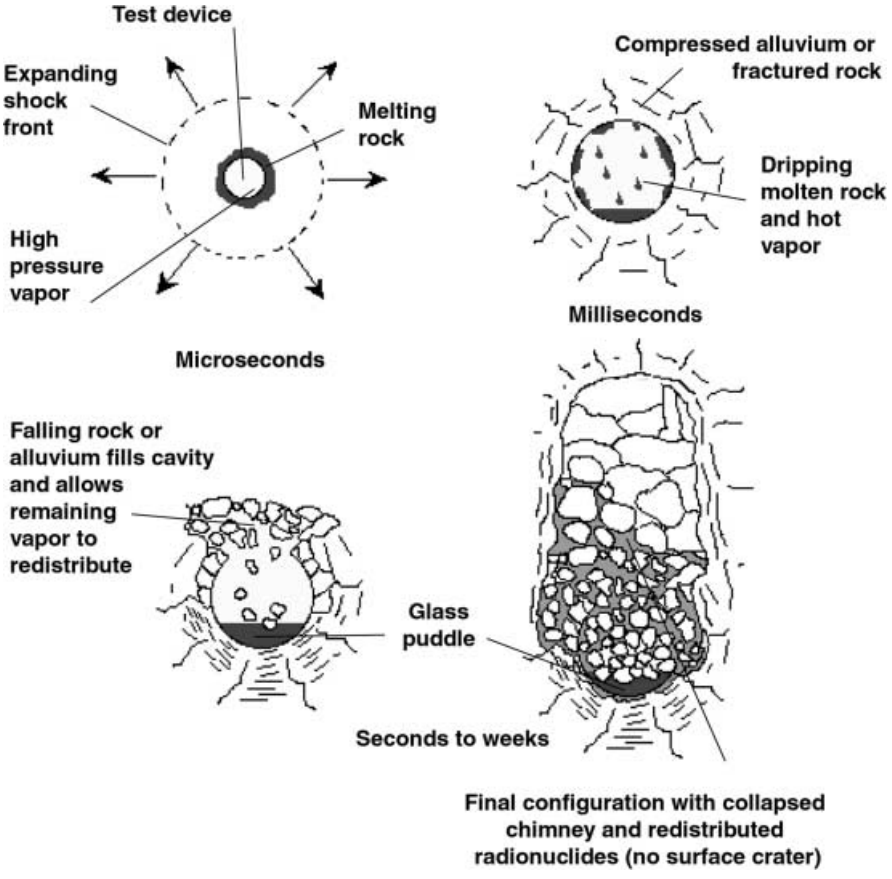

Fig. 1
Conceptual illustration of the phenomenology of an underground nuclear explosion showing accretion of melt glass puddle and redistribution of more volatile radionuclides, initially as vapor, later as condensate. Some non-condensable radionuclides may migrate further upwards

In the seconds and minutes following detonation, temperatures cool, gas pressures dissipate, and components of the cavity gas begin to condense in an order determined by their relative vapor pressures or boiling points. First among these are the rock and heavier radionuclide elements that, along with molten rock lining the cavity walls, tend to accumulate into a melt glass puddle at the bottom of the cavity. Within hours to days after the test, the overlying materials collapse into the cavity, creating a vertical "rubble" chimney that may extend as far as the ground surface, where a crater is formed. Portions of the collapsing materials can fall into the melt glass (Fig. 2). Groundwater will begin to refill the cavity at this time if the detonation point was initially under the water table.

Radionuclide distribution

Radionuclides associated with an underground nuclear explosion are derived from the original materials in the device, nuclear reactions connected with the explosion, and activation products created in the geologic medium. Complex dynamic processes, occurring milliseconds to hours after detonation, will control their initial chemical nature and spatial distribution. Most radionuclide vapors are retained in the cavity region during cavity expansion. This is because the uniform state of compression in the surrounding medium, generated by the outgoing shock wave and subsequent rebound of the geologic medium toward the detonation point, tends to close or seal potential pressure-driven escape pathways. Some exceptions to this have been noted, however, which could result in the "prompt injection" of small amounts of radionuclide vapors away from the cavity region (Nimz and Thompson 1992; Smith and others 1996).

During the cooling and condensation process, heavier radionuclides with higher boiling points such as ^{241}Am and ^{239}Pu condense first and become incorporated in the coalescing melt glass (Borg and others 1976; Smith 1995). Radionuclides with lower boiling points, such as tritium (^{3}H), ^{36}Cl, ^{22}Na, and ^{129}I, tend to condense later, usually along cavity wall and rubble surfaces within the cavity and in lower parts of the chimney, although some amounts can also be found in the melt phase (Borg and others 1976). This zone of radioactivity is often conceptualized as a spherical volume centered near the testing point whose "exchange" radius (Hoffman and others 1977), from 1.5 to 2 cavity radii, can be assessed from observations in drill-back wells (Borg and others 1976; Townsend 1994). Other radionuclides, such as ^{85}Kr, ^{90}Kr, or ^{137}Xe, will exist as non-condensable gases and may move beyond the exchange volume if conditions permit (Guell 1997). In general, vapor redistribution may be promoted by gas phase displacement associated with cavity collapse, buoyancy forces, and molecular diffusion, and will occur to the extent that unsaturated pore space is available for gases to move into. Some radionuclides, such as ^{90}Sr and ^{137}Cs, may be found well outside the melt zones because they are daughter products of short-lived gaseous precursors, such as ^{90}Kr and ^{137}Xe, respectively.

The inventory of radionuclides produced by a test can often be estimated from the test design and radiochemical diagnostic data, if available (e.g., Hoffman and others 1977). The partitioning of this inventory among the melt glass, exchange volume, and non-condensable gas fractions has also been estimated using diagnostic data from many tests and thermodynamic properties of the elements (IAEA 1998a). Similar data can be used to estimate the total mass of melt glass produced in a test as a function of the test yield. Olsen (1993) suggested that approximately 700 metric tons (t) of melt glass are produced per kiloton of test yield. Little is known about how radionuclides are locally concentrated within the melt glass or exchange volume, nor of their chemical state in the rubble following condensation and groundwater return. The melt phase is known to be a heterogeneous brecciated mixture of vesicular and massive glass (Fig. 2), often intermixed with rubble that has fallen in, all of which have different physicochemical properties and radionuclide contents (Wadman and Richards 1961; Townsend 1994; Smith 1995). The glass largely retains the chemical composition of the host rock (Tompson and others 1999). Within the rubble, condensed radionuclides may dissolve into returning pore water as steam condenses, or when groundwater returns to the cavity. They will form aqueous species according to local geochemical conditions, and may also partition onto reactive mineral phases or form precipitates according to constraints on their solubility. Non-condensable radionuclides may also become incorporated into returning pore waters, or may, depending on the rate of groundwater return and proximity to the unsaturated zone, move away from the cavity and chimney area altogether. Although some radionuclides have been measured in cavity waters sampled from drill-back wells (e.g., Hoffman and others 1977; Bryant 1992; Thompson 1996; Sawyer and others 1999), more accurate assessments of their true abundance and spatial distribution in the exchange volume are needed.

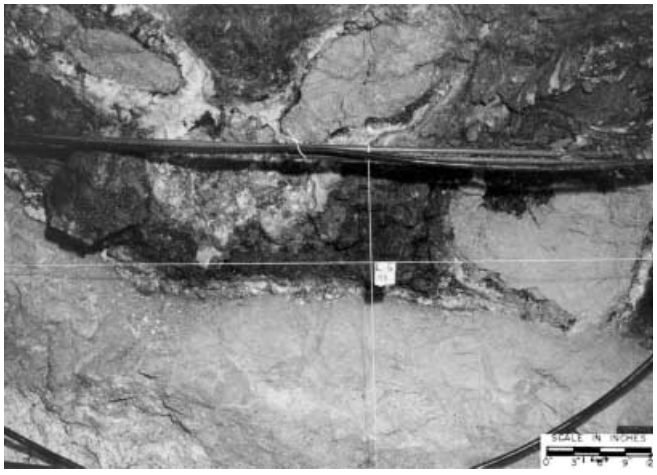

Fig. 2
In-situ photograph of the melt glass from an excavation at the RAINIER test (Wadman and Richards 1961). Large blocks of the host rock can be seen inside the melted glass zone. Vesicular zones (rich in bubbles) surround some of these inclusions. The photo shows a section of the pool about 2 m across. The zone is obviously heterogeneous in textural and hydrologic properties

Factors affecting radionuclide migration

Initial conditions for model analysis

Strictly speaking, the migration of test-related radionuclides begins at the time of test detonation, or "zero time", as their vapors are distributed and condensed inside the cavity and exchange volumes. However, the most logical starting point for examining radionuclide migration in groundwater will be in the days to months following zero time when groundwater returns to the cavity and chimney, and most of the complex dynamics initiated by the detonation have ended. Assuming the radionuclide inventory can be estimated, an "initial" state can be envisioned in which the respective fractions of the inventory mass are uniformly distributed within the melt glass and throughout an idealized spherical exchange volume surrounding the cavity. This approach assumes that estimates of the melt glass and exchange volume sizes are available and that local variation of radionuclide abundance within these areas will not be an important factor in ensuing calculations. In addition, the initial distribution of non-condensable radionuclides in this approach can only be roughly approximated, as noted by Guell (1999).

The release of radionuclides from this "initial" state will be influenced by groundwater flow and transport processes, variable temperature conditions, dissolution of melt glass, and geochemical behavior associated with speciation, sorption or precipitation reactions. These issues will be discussed below.

Groundwater flow

Relative to pre-test conditions, groundwater flow through the cavity and chimney areas may be modified by changes in formation permeability, or by transient phenomena associated with groundwater return and residual elevated temperatures (e.g., Knox and others 1965; Borg and others 1976; Burkhard and Rambo 1991; IAEA 1998b; Glascoe and others 2000; Maxwell and others 2000).

Changes in permeability will occur in the collapsed chimney as well as in the intact media adjacent to the cavity and chimney walls (Wadman and Richards 1961; McArthur 1963; Snoeberger and others 1973; Rozsa and others 1975; Borg and others 1976; Hansen and others 1981; IAEA 1998b). Within a collapsed chimney, these changes will depend on the type of collapsing material and the way in which it fills the cavity. Harder rock will typically break into larger fragments that easily bulk and create increased porosity and permeability. This would generally serve to increase the groundwater flow through these areas relative to pre-test conditions. In alluvial systems, collapsed material may be more "slumped" in nature, resulting in similar, or perhaps lower, permeability and porosity values. In one test, collapse phenomena have become coupled with the failure along nearby faults, leading to larger scale changes in the local groundwater flow regime (Pohlmann and others 1999).

In the intact media adjacent to the cavity and chimney, two types of permeability alteration may occur. In the immediate areas surrounding the bottom and sides of the cavity, a "crush-up" zone may be formed in which rock or even granular materials are pulverized and compressed into a rind of decreased permeability and porosity. When hard rock is present, a zone of increased shear fracturing may be created beyond the crush-up area with increased permeability and porosity. Permeability increases beyond these areas may also occur, but are considered to diminish rapidly with increasing radial distance. In general, our knowledge of these conditions has developed from observations of the disturbed areas in reentry tunnels and drill-back boreholes, as well as from some surface-based air-permeability tests over chimneys.

Outside of laboratory measurements on small melt glass fragments, the permeability and porosity of the in situ melt glass zone are not well known. These areas are clearly heterogeneous (Fig. 2) and potentially fractured, and will possess some degree of fracture permeability. Conversely, melt glass dissolution could lead to the formation of alteration minerals that could fill fracture spaces and reduce permeability.

Thermal effects

Residual heat from a nuclear test can last for years after detonation, well after groundwater returns to the chimney and cavity system (Maxwell and others 2000). The presence of test-related heat can alter the ambient groundwater flow and induce or reinforce vertical, buoyancy-driven flows, over and above what might be created from natural geothermal gradients alone (IAEA 1998b; Glascoe and others 2000; Maxwell and others 2000). Higher temperatures can also increase the rate of radionuclide release from the melt glass. The existence of upward groundwater flow in some locations has been postulated as a mechanism for allowing mobile radionuclides to rise to more permeable geologic zones and escape more quickly from a cavity and chimney system (Kersting and others 1999; Glascoe and others 2000).

The dissipation of test-related heat will be controlled by the rate of groundwater flow through the region and by thermal conduction. Because thermal conduction rates are relatively slow and well known, the length of time that test-related heat remains in a system can be used as a barometer of the overall rate of groundwater flow through the heated region, and, by inference, the region's permeability. This fact has been exploited by Maxwell and others (2000) to infer permeability contrasts among the melt glass, cavity, chimney, and the in-situ volcanic rock adjacent to the CHESHIRE test at Pahute Mesa at the Nevada Test Site. Figure 3 shows a series of temperature profiles that were calibrated to three temperature logs collected in the 6 years following the test along a diagonal borehole. These data show that the residual heat is initially concentrated in the melt glass proper and to a lesser degree in the volcanic rock just above the melt glass. The simulations suggest that the residual heat is effectively dissipated within 50 years after the test.

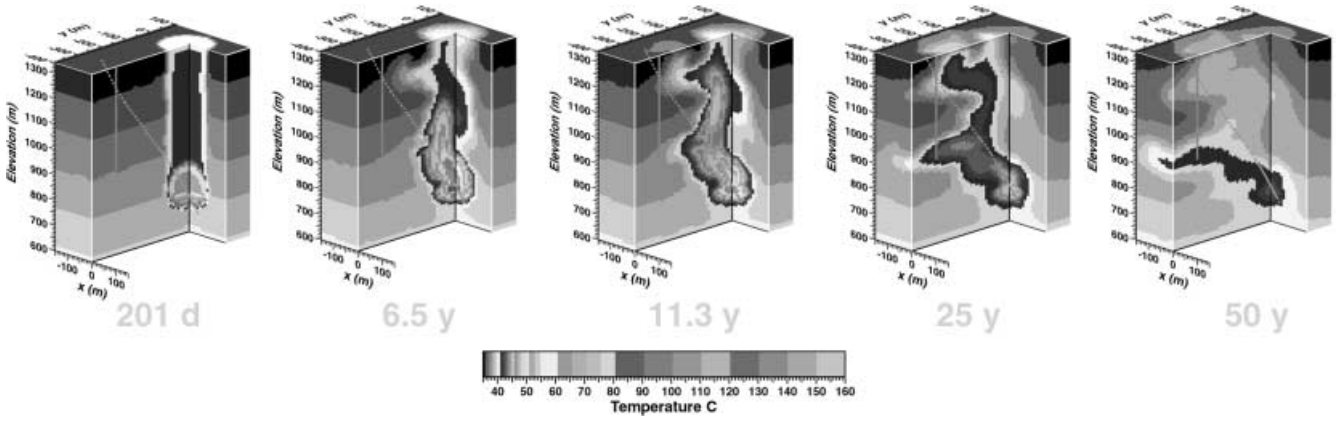

Fig. 3
Modeled temperature profiles at the CHESHIRE nuclear test, conducted at Pahute Mesa at the Nevada Test Site (Maxwell and others 2000), at 201 days, and 6.5, 11.3, 25, and 50 years after detonation. The test cavity is located in the lower part of the inside corner of the images. The top of the domain corresponds to the water table. Initially, higher temperatures induce upward moving water from buoyancy effects. Later, as the heat dissipates, buoyancy effects are overshadowed by horizontal flow gradients

Melt glass dissolution

The rate of release of radionuclides from the glass is proportional to the rate at which glass reacts with groundwater, and depends on temperature, pH, and fluid chemistry (Mazer 1987; Bourcier 1994). In general, the dissolution rates can be relatively slow compared with groundwater flow rates, albeit elevated early on as a result of residual high temperatures. Overall, melt glass can serve as a long-term source for radionuclides to enter the groundwater.

Geochemical processes

Radionuclides in the "exchange" volume may exist as aqueous species, sorbed species on the surfaces of reactive minerals and colloids, and as discrete solid phases and components of solid solutions. The state of a particular radionuclide will depend on radionuclide concentrations in solution, the presence of reactive minerals, and groundwater chemistry. The initial state of a radionuclide and the chemical processes that affect it will collectively influence radionuclide "release" from the exchange volume and subsequent mobility.

Retardation effects can be produced from surface complexation, ion exchange, or sorption reactions involving radionuclides and reactive minerals found (1) in the host rock or alluvium, (2) as coatings along fracture walls, or (3) as alteration minerals in the melt glass. In the latter case, radionuclides released from dissolving melt glass could be retarded or immobilized by the alteration minerals. In general, the types of reactive minerals and their quantity and spatial distribution will affect the overall retardation behavior. Colloidal particles can facilitate the migration of sorbing radionuclides, as observed by Kersting and others (1999). Precipitation and dissolution of solids containing radionuclides could also affect radionuclide mobility. Groundwater chemistry, including the redox state, will control aqueous speciation of radionuclides species and the solubility of radionuclide-bearing solids.

Example: the CAMBRIC test

As a more detailed example, we now consider a series of near-field model simulations involving radionuclide release away from the CAMBRIC nuclear test, which was conducted at Frenchman Flat at the NTS in 1965. Frenchman Flat, located in the southeast corner of NTS, is an intermountain basin formed by Tertiary-age faulting typical of the Basin and Range physiographic province. The working point and resulting test cavity are located in Quaternary–Tertiary alluvium, approximately 74 m beneath the ambient water table and 294 m beneath the ground surface (Fig. 4). The alluvium is composed of interbedded silts, clays, sands, and gravels derived largely from silicic volcanic rocks (tuff and rhyolitic lava). Alteration minerals include clinoptilolite, calcite, smectite, illite, and iron oxide, all of which possess sorptive potential. As reviewed by Hoffman and others (1977), Bryant (1992), and Tompson and others (1999), the CAMBRIC test had a small yield (0.75 kt), which produced a cavity and exchange volume with radii of approximately 10.9 and 18 m, respectively (Fig. 4). The melt glass is comprised of approximately 900 t of glass[1] which occupies a bulk region of 400 m^3 at the bottom of the cavity, assuming a 10% porosity (Tompson and others 1999). The chimney was known to extend above the water table, but not as far as the ground surface. A crush-up zone shown beneath the cavity in Fig. 4 was conceptualized as a low permeability unit in the simulations discussed below.

The CAMBRIC test was the subject of a long-term radionuclide migration experiment between 1975 and 1991, from which a considerable amount of pertinent chemical and physical data have been obtained (Hoffman and others 1977; Bryant 1992). The experiment involved the pumping of a nearby well in order to induce the elution of relatively mobile radionuclides such as ^{3}H, ^{36}Cl, ^{85}Kr, and ^{129}I. However, the simulations described in this example were limited to a subset of radionuclides and their migration under ambient (non-pumping) flow conditions. This

[1]Here, the mass of glass was chosen from the high end of a 700–1,200-t range of glass produced per kiloton of yield, which differs from the recommended lower end value, cited earlier from Olsen (1993).

approach was taken to develop a framework for estimating radionuclide release and migration at CAMBRIC and other tests at NTS (Tompson and others 1999), as well as to understand how local heterogeneity in the distribution of reactive minerals controls radionuclide migration at larger spatial scales.

Table 1 shows the derived inventory of radionuclides considered in the current simulations, decay corrected to zero time on 14 May 1965 (Tompson and others 1999). Because details of the initial radionuclide distribution are uncertain, these inventories were assumed to be uniformly distributed throughout the melt glass and exchange volumes according to the fractional distribution data in Table 2. Although a small 2% fraction of tritium is indicated to remain in an uncondensed gas phase, we assume that, for convenience, it is all dissolved within the groundwater in the pores of the exchange volume and melt glass. Prompt injection processes were not considered to be important at CAMBRIC.

Groundwater samples taken from below the cavity, after the test, were assumed to be representative of water chemistry in the vicinity of the CAMBRIC test. The composition of this water differed from waters sampled from within the cavity proper, but is similar to that of waters from volcanic aquifers elsewhere at NTS and was used in the simulations as given in Table 3. The redox state of the groundwater was assumed to be controlled by equilibrium with atmospheric oxygen, under which conditions radionuclides tend to be most mobile, leading to conservative estimates of migration.

Table 4 summarizes the aqueous species and solids considered in the simulations. Geochemical speciation calculations were used to identify potential radionuclide-bearing aqueous complexes in CAMBRIC groundwater, with provision for potential fluctuations in pH and bicarbonate concentration. Calculations were also used to identify the most likely radionuclide-bearing solids that might precipitate if saturation were achieved, either in the initial distribution, or during melt glass dissolution. Solid solutions and co-precipitation were not provided for in the models, so clinoptilolite and smectite solid solutions are represented by the calcium-rich compositional end members, Ca-clinoptilolite and Ca-beidellite, respectively.

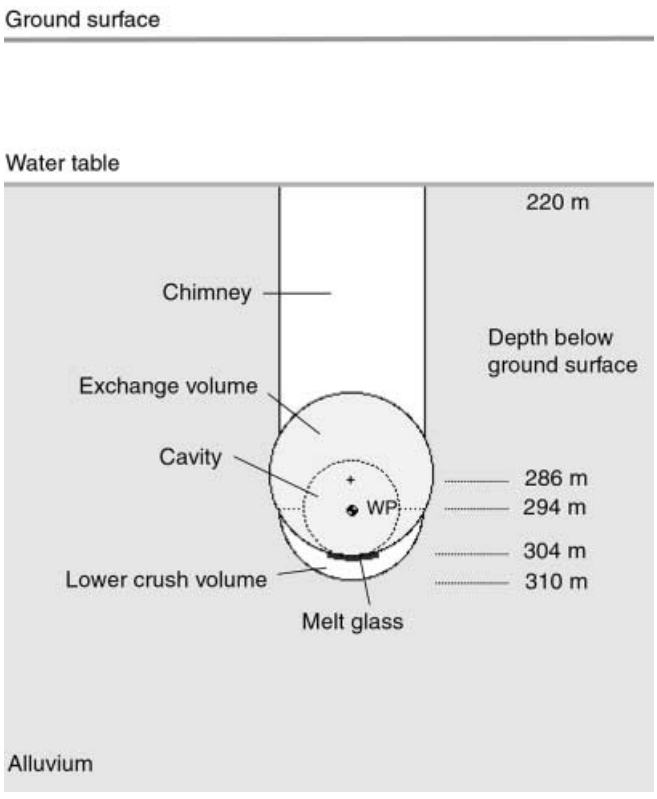

Fig. 4
Generic illustration of geologic units that comprise the cavity/chimney system in the CAMBRIC simulation model

Table 1
Half-life and derived inventory of selected radionuclides associated with the CAMBRIC test, decay corrected to zero time on 14 May 1965 (Tompson and others 1999)

Radionuclide	Half-life (years)	Derived inventory (mol)
^{3}H	12.3	2.04
^{90}Sr	28.8	3.44×10^{-3}
^{137}Cs	30.2	1.07×10^{-2}
^{155}Eu	4.7	8.46×10^{-5}
^{239}Pu	24,100	13.0
^{241}Am	432	5.19×10^{-2}

Table 2
Estimated distribution of selected radionuclides among the glass, rubble, gas, and groundwater at the CAMBRIC test (IAEA 1998a; Tompson and others 1999)

Radionuclide	Glass (%)	Rubble (%)	Gas (%)	Water (%)
^{3}H			2	98
^{90}Sr	25	75		
^{137}Cs	10	90		
^{155}Eu	95	5		
^{239}Pu	95	5		
^{241}Am	95	5		

Table 3
Ambient groundwater chemistry used in simulations

Constituent	Concentration (mg/l)
Na	63
K	8
Ca	16
Mg	4
Sr	0.24
HCO_3	177
Cl	16
SO_4	32
SiO_2	65
pH	8.0

Simulation approach

A streamline-based model was used to carry out reactive transport simulations. This model allows for the incorporation of detailed equilibrium and kinetic models to describe chemical interactions. Release of radionuclides from melt glass was modeled with a kinetic rate law for glass dissolution. Alteration minerals were allowed to precipitate when saturation limits were reached, and allowed to redissolve if dictated by changing chemical conditions. Surface complexation, ion exchange, and precipitation/dissolution were assumed to control release from the rubble/exchange volume and retardation in the alluvium. Although the framework mineralogy of the alluvium (e.g., quartz, feldspars) was assumed to be inert, surface-active (called reactive) minerals in the alluvium were allowed to precipitate and dissolve according to their saturation state, and alter the total sorptive capacity of the reactive minerals accordingly. See Tompson and others (1999) and below for more details.

Co-precipitation, solid solutions, colloid-facilitated transport, and changes in redox state were not considered in these simulations, nor was sorption to carbonates.

Melt glass dissolution model

At CAMBRIC, the melt glass has a rhyolitic composition with about 75 wt% silica, similar to the alluvium underlying Frenchman Flat (Schwartz and others 1984; Tompson and others 1999). The glass also contains radionuclides consistent with data in Tables 1 and 2.

In the absence of decay or mass transfer processes, the rate of release of radionuclides from the glass can be generally described by an equation of the form (Bourcier 1994):

$$\phi \frac{dc_j}{dt} = v_j r = v_j A_s k \left(\prod_i^N a_i^{p_i} \right) \left(1 - \frac{Q}{K} \right), \quad (1)$$

where c_j is the aqueous concentration of radionuclide j in groundwater, ϕ is the melt glass porosity, r is the intrinsic rate of glass dissolution per unit volume of bulk medium, and v_j is a stoichiometric coefficient describing the mole fraction of radionuclide j in the glass. The rate (r) is dependent on the specific surface area of the glass (A_s), a temperature-dependent rate coefficient (k), a dimensionless product factor dependent on the activities (a_i) of N catalytic or inhibitive aqueous species, and an affinity term ($1–Q/K$), which provides for a slow-down in the rate resulting from saturation effects.

The rate coefficient and pH dependence (a_{H+}) in Eq. (1) were determined from experimental data (Mazer 1987). Groundwater was assumed to buffer the pH at 8 and the concentration of aqueous silica [SiO_2 (aq)] at 65 mg/l. In the affinity term, Q and K are the activity product and equilibrium constant for the glass dissolution reaction, respectively. In the following simulations, we assume that Q is the activity of SiO_2 (aq), and K is the solubility product for amorphous silica. These parameters provide a conservative estimate of glass dissolution rate. The temperature was assumed fixed at 250 °C.

One of the critical parameters in (1) is the specific melt glass surface area (A_s). As discussed in Tompson and others (1999), our nominal value of 0.5 cm^2/g (or about 118 m^2/m^3) was estimated from reactive surface area measurements of fractured glass in waste form canisters (Baxter 1983). This is, at best, an lower bound value because the real surface area in the heterogeneous melt glass (Fig. 2) is likely much larger (Tompson and others 1999). Although measured data on melt glass surface areas is largely non-existent at his time, several ongoing experiments are being performed to get a better handle on its magnitude in real and analog melt glass samples.

Surface complexation and ion exchange

Surface complexation, ion exchange, precipitation, and dissolution were assumed to control radionuclide release from the exchange volume and retardation in the alluvium. Reactive minerals in the alluvium include goethite (iron oxide), clinoptilolite (zeolite), and smectite and illite/muscovite (clays). A one-site non-electrostatic surface complexation model was used to describe Pu and Sr sorption onto goethite. Ion exchange was modeled using the ideal Vanselow convention. Exchange was considered between Sr and Ca on clinoptilolite, Ca, Mg, and Sr on smectite, and Cs, Na, and K on illite/muscovite (Tompson and others 1999). Surface areas and cation exchange capacities were taken from the literature in the absence of site-specific data (Tompson and others 1999).

Table 4
Aqueous species and solids considered in the reactive transport simulations. Tritium (^3H) was only used in a calibration test and is not included here

H^+	OH^-	Na^+	Ca^{2+}
K^+	Mg^{2+}	O_2(aq)	Fe^{2+}
Fe^{3+}	$Fe(OH)_3$(aq)	$Fe(OH)_4^-$	$Fe(OH)_2^+$
Al^{3+}	AlO_2^-	SiO_2(aq)	$HSiO_3^-$
HCO_3^-	CO_3^{2-}	SO_4^{2-}	Cl^-
Cs^+			
Sr^{2+}			
Eu^{3+}	$EuOHCO_3$(aq)	$Eu(OH)_2CO_3^-$	$EuOH(CO_3)_2^{2-}$
Am^{3+}	$AmCO_3^+$	$Am(CO_3)_2^-$	$Am(OH)_2^+$
Pu^{4+}	$PuO_2(CO_3)_2^{2-}$	$PuO_2(CO_3)_3^{4-}$	$PuO_2CO_3^-$
$PuO_2(OH)_2$(aq)	PuO_2^{2+}	PuO_2^+	
Melt glass	Inert matrix (quartz, feldspar)		
Muscovite	Ca-clinoptilolite	Ca-Beidellite	Goethite (FeOOH)
β-cristobalite (SiO_2)	Calcite ($CaCO_3$)		
$EuOHCO_3$	$AmOHCO_3$	$PuO_2(OH)_2\ H_2O$	

Given the lack of readily available sorption data for Eu and Am at the time of this work, Eu and Am were not assumed to participate in any sorption reactions. Therefore, they migrated as tracers in the simulations in the absence of retarding mechanisms.

Hydrologic flow and transport at CAMBRIC

A simple, steady state groundwater flow model in the vicinity of the CAMBRIC test was developed as an initial basis to forecast radionuclide migration away from the cavity and chimney regions. Thermal alterations to the flow field, as shown in Fig. 3, were not considered because elevated temperatures were not noticed during the migration study (Hoffman and others 1977) and the test was atypically small in terms of its yield. The model domain is comprised of a 450-m-long by 360-m-wide by 210-m-deep prismatic block "carved" out of the local alluvium just beneath the water table. It includes the cavity and chimney features of the CAMBRIC test, and encompasses the region influenced by the long-term migration experiment (Hoffman and others 1977; Bryant 1992). The domain was oriented such that its longer side is collinear with the topographical gradient and principal direction of geologic deposition, as well as the apparent (ambient) horizontal hydraulic gradient (about 0.001 in magnitude).

In-situ alluvium was represented by a series of horizontal layers with distinct hydraulic and chemical properties. Within each layer, non-uniform distributions of scalar-valued hydraulic conductivity were specified according to a lognormal correlated Gaussian random field model to reflect observed variability in available (yet sparse) conductivity data. Additional experimental data are required to reduce uncertainty in the parametric data required for the model (ln K variance and spatial correlation scales) and its overall applicability (Tompson and others 1999). In general, mean conductivity values in the layers ranged from 0.2 to 10 m/day, with some localized extreme values reaching over 50 m/day. Correlation scales ranged from 6 (vertical) to 24 m (horizontal in the direction of flow), while ln K variances were approximately 2.3. The porosity was assumed to be a uniform value of 0.4. Hydraulic conductivities in the cavity, chimney, and melt glass zones were assumed to be smaller than those found in the surrounding media. Because the material in the cavity and chimney represents slumped or collapsed alluvium, smaller values seemed appropriate (Borg and others 1976; Tompson and others 1999), although this would tend to reduce flow through the radioactive exchange volume (see related discussion in section Factors affecting radionuclide migration). The conductivity of the glass and crush-up zones was assumed to be quite small (0.04 m/day), with a porosity of 0.1 (Borg and others 1976). The principal chemical properties of the alluvium and cavity/chimney rubble were specified in terms of the abundance of reactive minerals (Table 5), and the specific properties of the melt glass.

Steady flow in the system was based upon the solution of the traditional, steady porous flow equations

$$\nabla \cdot (\phi v) = 0 \tag{2a}$$

and

$$\phi v = -K \cdot \nabla h \tag{2b}$$

where ϕ is the medium porosity, v is the average seepage velocity, h is the hydraulic head, and K is an isotropic hydraulic conductivity. Flow was induced through specification of a small fixed hydraulic gradient of 0.001 across the longitudinal axis of the domain, with no-flow lateral boundaries. This is consistent with conditions in Frenchman Flat. The flow solution was developed on a regular, fixed three-dimensional grid using the model Parflow (Tompson and others 1998). An earlier calibration of this model incorporated a pumping well to reflect the 16-year migration experiment and the subsequent capture of the tritium inventory shown in Tables 1 and 2 (Tompson and others 1999). The calibration step allowed the hydraulic conductivity values to be adjusted so that the breakthrough of tritium at the well could be effectively reproduced. Remaining simulations incorporated ambient flow conditions only in order to look at long-term releases, and they focused on radionuclides other than tritium.

Streamline transport model

Reactive transport simulations were accomplished with a streamline-based transport model. In this approach, a three-dimensional transport problem is recast into a large number of independent one-dimensional reactive transport simulations that correspond in a one-to-one fashion to a large number of streamlines that have been extracted from the simulated three-dimensional flow field (Thiele and others 1996; Yabusaki and others 1998; Crane and Blunt7 1999; Tompson and others 1999;). Figure 5 shows a portion of the domain and a series of streamlines that pass through the exchange volume and melt glass zones in the model. The streamline mapping procedure is, in some sense, a regridding process tailored specifically for transport simulations. The procedure used to select the streamlines was

Table 5
Volume percentages of reactive minerals used in the simulations for the alluvium/exchange volume and melt glass. Reactive or inert medium configurations are used at different spatial locations in transport simulations (see text). Quartz and feldspar assigned to "inert matrix". Muscovite is a proxy for illite

Phase	Reactive medium	Inert medium	Melt glass
Glass	0	0	90
Inert matrix	47	60	0
Ca-clinoptilolite	5	0	0
Ca-beidellite	5	0	0
Calcite	1	0	0
Muscovite	1	0	0
Goethite	1	0	0
Pore space	40	40	10

constrained by a desire to (1) use streamlines passing only through the initially-contaminated regions, as opposed to the entire domain, to focus all computational effort on the migrating radionuclides; and (2) have at least one streamline passing through each grid block inside of the contaminated zone to provide a numerical basis to "pick up" all of the mass comprising the initial inventory. Altogether, 809 streamlines were extracted from the flow simulation (Fig. 5) for the transport model. This selection approach did not ensure that all grid-blocks down-gradient of the initially contaminated region had streamlines passing through them. However, such grid blocks, should they exist, would likely be associated with very low conductivities and a lack of streamline resolution in these regions would be less important from an overall migration perspective.

The streamline approach, in general, does not allow for mass transfer between streamlines, as would occur from transverse dispersion and diffusion processes. This is recognized as an approximation, although the errors incurred would be smaller in heterogeneous and advectively dominated problems such as this, where the resolution of the flow model is relatively large ($\Delta x_i \sim 2$ m) and allows for the larger scale dispersion or spreading effects to be directly simulated (Gelhar 1993). In addition, the streamline approach is best suited for use in steady flow problems. Transient flows, as may be induced by thermal effects or changing porosity conditions, pose additional challenges that may (Batycky and others. 1997) or may not be successfully approximated with a streamline method.

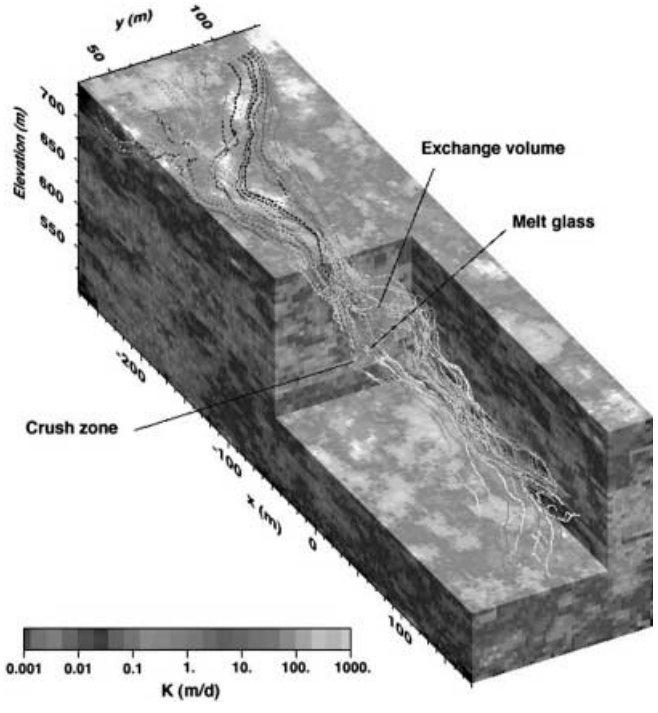

Fig. 5
Portion of the flow model domain, with flow moving from the upper left to lower right. *Shading* indicates relative values of hydraulic conductivity within the range of .01–100 m/day. Selected streamlines shown passing through the exchange volume and melt glass zones

Along each streamline, the one-dimensional reactive transport simulations were made using the GIMRT model (Steefel and Yabusaki 1996), reconfigured in a "time-of-flight" formulation (Tompson and others 1999; Thiele and others 1996):

$$\phi\frac{\partial\left(u_j+u_j^{im}\right)}{dt}+\phi\frac{\partial u_j}{d\tau}-\phi\frac{\partial}{d\tau}\left(\frac{D}{V^2}\frac{\partial u_j}{d\tau}\right)$$
$$=-\sum_{m=1}^{N_m}v_{jm}r_m-\lambda_j\phi\left(u_j+u_j^{im}\right)+\lambda_k\phi\left(u_k+u_k^{im}\right) \quad (3)$$

In this expression, the curvilinear spatial coordinate along the streamline has been transformed into a time of flight variable (τ). The concentrations u_j and u_j^{im} represent the total mobile and immobile concentrations of radionuclide j, each being linear combinations of primary and secondary species that are related through equilibrium mass action (sorption) relationships (Thiele and others 1996; Tompson and others 1999). Local longitudinal dispersion (D) was not considered in the current work.

The rate terms on the right-hand-side of Eq. (3) represent accumulation of radionuclides from dissolution of melt glass or other solids, loss through precipitation of solids (Table 4), or gains and losses from radioactive decay. Rate laws for mineral kinetics similar to (1) are used here; surface areas and kinetic parameters for processes other than melt glass dissolution are discussed by Tompson and others (1999). If species j is a member of a radionuclide decay chain, then λ_j represents its decay rate (related to its half-life by $t_{1/2}=\ln 2/\lambda$), whereas λ_k represents its in-growth rate from the decay of its parent nuclide k. In this work, the effects of radioactive in-growth are not needed, whereas radioactive decay is incorporated in an approximate, ex post facto manner by appropriate adjustment of concentrations at the end of a simulation. Cumulative impacts of radionuclide decay and daughter product in-growth accrued over the course of a simulation could not be treated in GIMRT at the time of the simulations.

Simulations along each streamline are initiated by assigning the initial aqueous chemistry (Table 3) and appropriate mineralogy (see below) along the entire line. This may include the melt glass for those portions of the lines passing through the glass volume. For those lines passing through the exchange volume, the applicable radionuclide inventory is assigned to the appropriate section of the line and partitioned among the water and reactive minerals as conditions dictate.

Reactive mineral heterogeneity

The reactive minerals shown in Table 5 were determined from mineralogic descriptions of samples from two boreholes in the vicinity of CAMBRIC. These descriptions indicate that the mineralogic abundance is spatially variable. Based upon the observation that zeolites are in greatest abundance in a layer with the lowest hydraulic conductivity, we assumed that hydraulic conductivity is inversely correlated with reactive mineral abundance. This assumption was used in a series of sensitivity simulations to gauge the effects of the mineralogic distribution on the

overall elution of radionuclides out of the system. These results suggest that spatially variable distributions of reactive minerals can dramatically impact the mobility of radionuclides (Tompson and Jackson 1996). We also simulated the impact of an increased glass dissolution rate, as might be produced by a larger melt glass surface area (A_s) or a larger rate coefficient (k) in Eq. (1).

Using the terminology of Tompson and others (1999), mineralogic model 10 assigns the reactive medium specification (Table 5) uniformly to all points in the model domain. Model 11 assigns an inert mineral specification (Table 5) uniformly to all points in the model domain. Model 12 assigns the reactive specification to the 1% of the domain with the lowest conductivity values, with an inert specification elsewhere. Model 10a was similar to model 10, although the nominal goethite surface area was reduced to 50 m^2/g from 600 m^2/g. Model 13a assigned the reactive medium specification with the reduced goethite surface area (as in 10a) to 80% of the domain with the lowest conductivity values. Model 10d was the same as model 10a, except that the glass dissolution rate was increased by a factor of 100. The increased rate can be interpreted as being caused by a larger specific glass surface area (see section Simulation approach) or a combination of changes in the other factors that comprise the glass dissolution rate in Eq. (1).

Some simulation results

Figure 6 shows the total flux of the total Eu, Am, Pu, Sr, and Cs out of the domain over a 600-year period, as integrated over all streamlines for mineralogic model 10.

Figure 7 shows a 3-D snapshot of the total Eu plume after 100 years. Because its lack of retardation, Am shows the most significant breakthrough, with the 5% exchange volume fraction eluting first and the remaining signal coming from slower dissolution of the melt glass. Although not retarded either, the Eu breakthrough is much less notable because of radioactive decay (Fig. 7). The Pu, Sr, and Cs fluxes should be considered as "0" because their corresponding concentrations are all below small input background levels required in GIMRT. Radionuclide precipitation did not occur in this simulation.

Figure 8 shows the total flux of the same radionuclides corresponding to mineralogic model 11, in which no reactive minerals were present in the domain. Although the Am and Eu results are unchanged, Pu, Sr, and Cs now exhibit breakthrough because of their increased mobility

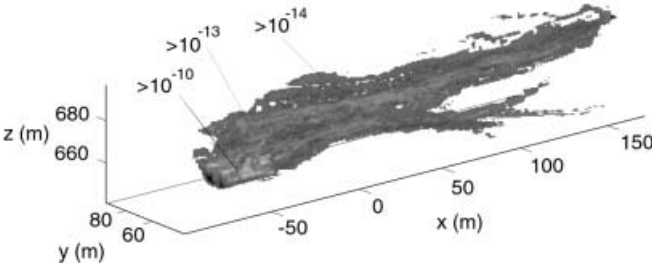

Fig. 7
3-D perspective of decay-corrected total Eu at 100 years (assuming Eu was not retarded by chemical reactions) for mineralogic model 10. Molar concentrations $>10^{-14}$ are in blue; $>10^{-13}$, in aqua, and $>10^{-10}$ in yellow. Eu originally in the exchange volume has been flushed out and decayed, whereas Eu contained in the melt glass is still entering the domain

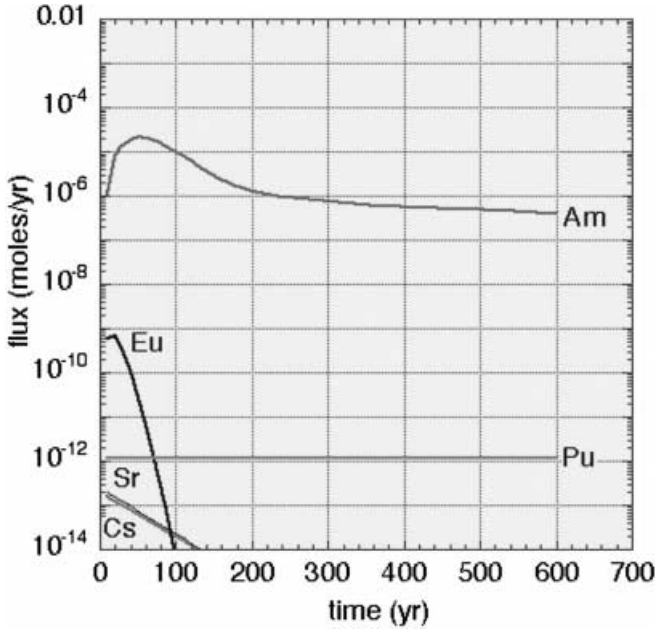

Fig. 6
Integrated, decay-corrected flux profiles (mol/year) for total Cs, Sr, Eu, Pu, and Am out of the model domain for mineralogic model 10

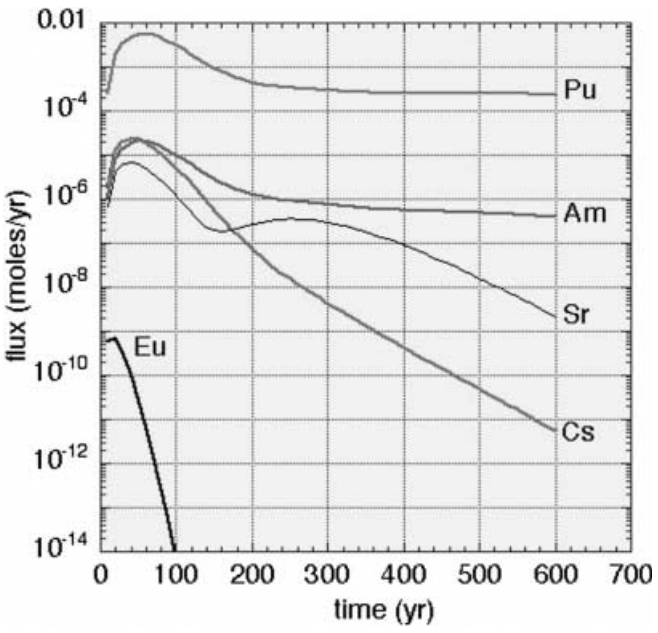

Fig. 8
Integrated, decay-corrected flux profiles (mol/year) for total Cs, Sr, Eu, Pu, and Am out of the model domain for mineralogic model 11

in the system. The only chemical processes affecting elution out of the domain in this simulation are melt glass dissolution and radioactive decay. Most elution curves show the early release of the exchange volume components, followed by a slower release from the glass. Pu shows the largest release rate because its inventory (Table 1) was the largest of the radionuclides considered. Figure 9 shows the total flux of total Pu for each of the mineralogic models considered. The small fraction of reactive minerals in model 12 slightly affected the latter end of the elution curve when compared with model 11. Comparison of model 10a with model 10 shows breakthrough occurs with reduction of the goethite surface area, despite the fact that the reactive minerals are uniformly distributed in both models. Greater elution occurs in model 13a relative to 10a because the reactive mineral specification is now constrained to be in the 80% of the alluvium with the lowest hydraulic conductivity. Faster flow pathways in higher conductivity regions with no reactive minerals contribute to the increased mobility of Pu. Finally, in comparing model 10a with 10d, a dramatic increase in the Pu elution arising from the increased melt glass dissolution rate is observed. The elution profile flattens in model 10d when $PuO_2(OH)_2\ H_2O$ reaches saturation and precipitates in the melt glass zone, essentially limiting the aqueous Pu release.

Figure 10 shows two 3-D snapshots of the total Pu plume after 600 years corresponding to mineralogic models 13a and 10d, respectively. The larger glass dissolution rate used in mineralogic model 10d clearly promotes increased Pu release relative to that in mineralogic model 13a. However, the slightly increased mobility of Pu in mineralogic model 13a, because of the lack of reactive minerals in some portions of the alluvium, is also evident.

Conclusions

Estimating the rate of radionuclide release into groundwater from underground nuclear tests can be a challenging task. Our near-field simulations indicate that the cavity, chimney, and melt glass can act as significant sources of radionuclides for hundreds to thousands of years, or more. Important processes controlling the rates of radionuclide introduction into groundwater include melt glass dissolution and chemical retention effects associated with sorption on reactive minerals. Elution was particularly sensitive to the abundance and distribution of reactive minerals in the system and the dissolution rate of melt glass. Ultimately, these factors need to be effectively understood, addressed, and represented in larger scale regional models designed for risk analyses and regulatory management (USDOE 1997a).

The streamline modeling approach proved to be an exceptionally useful and flexible technique for studying this problem. It allowed a highly resolved 3-D reactive transport problem to be decomposed into a large, yet tractable, number of 1-D reactive transport problems, whose results could later be recombined into a 3-D solution. Solutions were assembled using less computer time and allowed for difficult aspects of the problem to be solved more quickly. Analysis of preliminary 1-D solutions allowed for faster benchmarking of specific sensitivity and design issues, as well as for diagnosis and interpretation of particular transport and reaction behavior before the remaining streamline simulations were performed.

Efforts are underway to measure reactive glass surface areas from retrieved melt glass samples and analog volcanic glasses, as well as to better characterize the mineralogy and heterogeneity of alluvium. Data collection

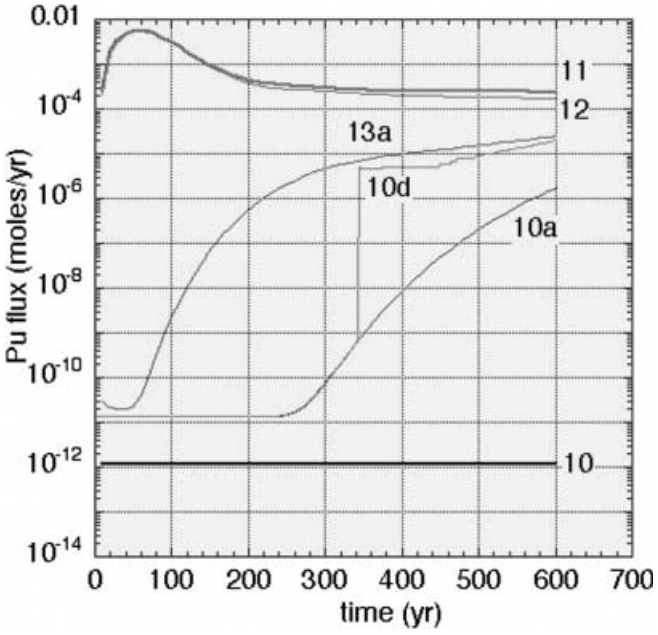

Fig. 9
Integrated, decay-corrected flux profiles (mol/year) for total Pu corresponding to all mineralogic models (10, 11, 12, 10a, 10d, 13a)

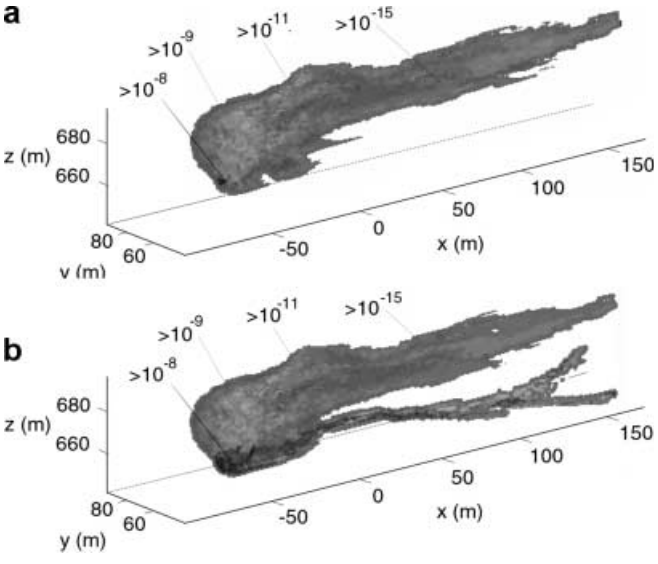

Fig. 10
3-D perspectives of decay-corrected total Pu at 600 years for mineralogic models 13a (*top*) and 10d (*bottom*). Molar concentrations $>10^{-15}$ are in blue; $>10^{-11}$, in green, $>10^{-9}$ in yellow, and $>10^{-8}$ in orange/yellow

efforts are being considered to better characterize in-situ radionuclide concentrations for monitoring and model validation purposes, as well as better characterizing their sorptive and colloidal transport properties. Field data are critically important for better understanding the relevant physical and chemical processes in the system, as well as for calibrating and validating predictive models.

Acknowledgements This work was conducted under the auspices of the US Department of Energy by the University of California, Lawrence Livermore National Laboratory under contract W-7405-Eng-48. This work was funded by the Underground Test Area Project, US Department of Energy, Nevada Operations Office.

References

Batycky RP, Blunt MJ, Thiele MR (1997) A 3D field-scale streamline-based reservoir simulator. Soc Petrol Eng Reservoir Eng 12(4):246–254

Baxter RG (1983) Description of defense waste processing facility reference waste form and container, Savannah River. Aiken, SC, DP-1606, rev. 1

Borg I, Stone R, Levy HB, Ramspott LD (1976) Information pertinent to the migration of radionuclides in ground water at the Nevada Test Site. Part 1: review and analysis of existing information. Lawrence Livermore National Laboratory, Livermore, CA (UCRL-52078)

Bourcier WL (1994) Waste glass corrosion modeling: comparison with experimental results. Mater Res Soc Symp Proc 333:69–82

Bryant EA (1992) The CAMBRIC migration experiment: a summary report, Los Alamos National Laboratory, Los Alamos, NM (LA-12335-MS)

Burkhard NR, Rambo JT (1991) One plausible explanation for water mounding. In: Proceedings of the 6th Symposium on Containment of Underground Nuclear Explosions, CONF-9109114, vol 2. Lawrence Livermore National Laboratory, Livermore, CA

Crane MJ, Blunt MJ (1999) Streamline-based simulation of solute transport. Water Resour Res 35(10):3061–3078

Gelhar LW (1993) Stochastic subsurface hydrology. Prentice Hall, Englewood Cliffs

Germain LS, Kahn JS (1968) Phenomenology and containment of underground nuclear explosions, UCRL-50482. Lawrence Livermore National Laboratory, Livermore, CA

Glascoe A, Olson J, Lu G, McGraw MA, Lichtner PC, Wolfsberg AV (2000) Radionuclide transport from an underground nuclear test in the presence of residual heat and colloids. In: Bentley L, Sykes J, Brebbia C, Gray W, Pinder G (eds) Computational methods in water resources XIII, vol. 1. AA Balkema, Rotterdam, pp 357– 364

Guell MA (1997) Subsurface transport of radionuclides at the Nevada Test Site. PhD Thesis, Department of Civil and Environmental Engineering, University of California, Berkeley

Hansen ME, Terhune RW, McKee CR (1981) Explosion phenomenology and permeability enhancement in porous media, UCRL-85811. Lawrence Livermore National Laboratory, Livermore, CA

Hoffman DC, Stone R, Dudley WW Jr (1977) Radioactivity in the underground environment of the CAMBRIC nuclear explosion at the Nevada Test Site, LA-6877-MS. Los Alamos National Laboratory, Los Alamos, NM

IAEA (1998a) The radiological situation at the atolls of Mururoa and Fangataufa. Technical report, vol 3. Inventory of radionuclides underground at the atolls, IAEA-MFTR-3. International Atomic Energy Agency, Vienna

IAEA (1998b) The radiological situation at the atolls of Mururoa and Fangataufa. Technical report, vol 4. Releases to the biosphere of radionuclides from underground nuclear weapons tests at the atolls, IAEA-MFTR-4. International Atomic Energy Agency, Vienna

IAEA (1998c) The radiological situation at the atolls of Mururoa and Fangataufa. Technical report, vol 6. Doses due to radioactive materials present in the environment or released from the atolls, IAEA-MFTR-6. International Atomic Energy Agency, Vienna

Kersting AB, Efurd DW, Finnegan DL, Rokop DJ, Smith DK, Thompson JL (1999) Migration of plutonium in groundwater at the Nevada Test Site. Nature 397(6714):56–59

Knox JB, Rawson DE, Korve JA (1965) Analysis of a groundwater anomaly created by an underground nuclear explosion. J Geophys Res 70(4):823–835

McArthur RD (1963) Geologic and engineering effects, the HARDHAT event (preliminary), GN 1-63, February. Lawrence Livermore National Laboratory, Livermore, CA

Maxwell RM, Tompson AFB, Rambo JT, Carle SF, Pawloski GA (2000) Thermally induced groundwater flow resulting from an underground nuclear test. In: Bentley L, Sykes J, Brebbia C, Gray W, Pinder G (eds) Computational methods in water resources XIII, vol. 1. AA Balkema, Rotterdam, pp 45–50

Mazer JJ (1987) Kinetics of glass dissolution as a function of temperature, glass composition, and solution pH. PhD Thesis, Northwestern University

Nimz GJ, Thompson JL (1992) Underground radionuclide migration at the Nevada Test Site. DOE/NV-246, UC-703, US Department of Energy, Nevada Field Office

Ogard AE, Thompson JL, Rundberg RS, Wolfsberg K, Kubic PW, Elmore D, Bentley HW (1988) Migration of chlorine-36 and tritium from an underground nuclear test. Radiochim Acta 44/45:213–217

Olsen CW (1993) Site selection and containment evaluation for LLNL nuclear events. In: Proceedings of the 7th Symposium on Containment of Underground Nuclear Explosions, vol 1, CONF-9309103. Lawrence Livermore National Laboratory, Livermore, CA

Pawloski GA (1999) Development of phenomenological models of underground nuclear tests on Pahute Mesa, Nevada Test Site, BENHAM and TYBO, UCRL-ID-136003. Lawrence Livermore National Laboratory, Livermore, CA

Pohll G, Hassan A, Chapman J, Papelis C, Andricevic R (1999) Modeling ground water flow and radioactive transport in a fractured aquifer. Ground Water 37(5):770–784

Pohlmann K, Chapman J, Hassan A, Papelis C (1999) Evaluation of groundwater flow and transport at the FAULTLESS underground nuclear test, Central Nevada Test Area, Publication 45165. Desert Research Institute, University and Community College System of Nevada, Las Vegas

Rozsa R, Snoeberger D, Baker J (1975) Permeability of a nuclear chimney and surface alluvium, UCID-16722. Lawrence Livermore National Laboratory, Livermore, CA

Sawyer DA, Thompson JL, Smith DK (1999) The CHESHIRE migration experiment: a summary report, LA-13555-MS. Los Alamos National Laboratory, Los Alamos, NM

Schwartz L, Piwinskii A, Ryerson F, Tewes H, Beiringer W (1984) Glass from underground nuclear explosions. J Noncrystall Solids 67:559–591

Smith DK (1995) Characterization of nuclear explosive melt debris. Radiochim Acta 69:157–167

Smith DK, Nagle RJ, Kenneally JM (1996) Transport of gaseous fission products adjacent to an underground nuclear test cavity. Radiochim Acta 73:177–183

Snoeberger DF, Baker J, Morris CJ (1973) Measurements and correlation analysis for nuclear chimney permeability, UCID-16302. Lawrence Livermore National Laboratory, Livermore, CA
Steefel CI, Yabusaki SB (1996) OS3D/GIMRT, Software for modeling multicomponent and multidimensional reactive transport. User manual and programmer's guide, version 1.0, PNL-11166. Pacific Northwest National Laboratory, Richland, WA
Thiele MR, Batycky RP, Blunt MJ, Orr FM (1996) Simulating flow in heterogeneous systems using streamtubes and streamlines. Soc Petrol Eng Reservoir Eng 10:5–12
Thompson JL (1996) Radionuclide distribution in a nuclear test cavity: the BASEBALL event. Radiochim Acta 72:157–162
Tompson AFB, Jackson KJ (1996) Reactive transport in heterogeneous systems: an overview. Rev Mineral 34:269–310
Tompson AFB, Falgout RD, Smith SG, Bosl WJ, Ashby SF (1998) Analysis of subsurface contaminant migration and remediation using high performance computing. Adv Water Resour 22(3):203–221
Tompson AFB, Bruton CJ, Pawloski GA (eds) (1999) Evaluation of the hydrologic source term from underground nuclear tests in Frenchman Flat at the Nevada Test Site: the CAMBRIC test, UCRL-ID-132300. Lawrence Livermore National Laboratory, Livermore, CA
Townsend DR (1994) RED HOT reentry. A report on the results of four phases of reentry mining and drilling conducted by the defense nuclear agency between 1981 and 1985, Raytheon Services Nevada, NTS Operations, Geology/Hydrology section (TSP:DGP:066:95), December
US Congress, Office of Technology Assessment (1989) The containment of underground nuclear explosions, OTA-ISC-414. US Government Printing Office, Washington, DC
USDOE (2000) United States nuclear tests: July 1945 through September 1992. DOE/NV-209; Rev 15, US Department of Energy, Nevada Operations Office, Las Vegas, NV
USDOE (1997a) Regional groundwater flow and tritium transport modeling and risk assessment of the underground test area, Nevada Test Site, Nevada. DOE/NV-477, US Department of Energy, Nevada Operations Office, Environmental Restoration Division, Las Vegas, NV
USDOE (1997b) Shaft and tunnel nuclear detonations at the Nevada Test Site: development of a primary database for the estimation of potential interactions with the regional groundwater system. DOE/NV-464, US Department of Energy, Nevada Operations Office, Las Vegas, NV
Wadman RE, Richards WD (1961) Postshot geologic studies of excavations below RAINIER ground zero. UCRL-6586, Lawrence Livermore National Laboratory, Livermore, CA
Wild JF, Goishi W, Meadows JW, Namboodiri MN, Smith DK (1998) The LLNL Nevada Test Site underground radionuclide source-term inventory. In: Shapiro CS (ed) Atmospheric nuclear tests – environmental and human consequences. NATO ASI Series, Springer, Berlin Heidelberg New York, pp 69–77
Yabusaki SB, Steefel CI, Wood BD (1998) Multidimensional, multicomponent, subsurface reactive transport in nonuniform velocity fields: code verification using an advective reactive streamtube technique. J Contam Hydrol 30:299–331